TECHNICAL MEMORANDUMS

NATIONAL ADVISORY COMMITTEE FOR AERONAUTICS

No. 598

RIVETING IN METAL AIRPLANE CONSTRUCTION

By Wilhelm Pleines

PART III

From Luftfahrtforschung, Vol. VII, No. 1, April 30, 1930

Washington
December, 1930

NATIONAL ADVISORY COMMITTEE FOR AERONAUTICS

TECHNICAL MEMORANDUM NO. 598

RIVETING IN METAL AIRPLANE CONSTRUCTION*

By Wilhelm Pleines

PART III

Strength of Riveted Joints in Duralumin (continued)

Test Installation and Arrangement

Test arrangement and test program.- We selected a double shear bolted joint (to conform with the double shear one-rivet riveted joint) with one bolt, the butt straps and the bolt of steel, the rivet plate of duralumin (Fig. 91).

In deciding on the material for butt straps and bolt, we intended the dimensions of these pieces to be large enough so as to remain below the yield point when the plate failed under maximum crushing pressure. We used high tensile steel (σ_B = ~115.0 kg/mm^2, Brinell hardness). Another factor in this decision was that for duralumin the ratio $\frac{\text{shearing strength}}{\text{tensile strength}}$ is much lower than in iron and steel (about 0.70 - 0.8 by steel and iron as compared to 0.6 - 0.65 for duralumin), and that the ratio of compression strength to tensile strength in duralumin is much higher than in steel.

Pietzker, ("Strength of Ships," Berlin 1911, published by Mittler & Co.), not without cause, points out that conditions

*"Nietverfahren im Metallflugzeugbau." From Luftfahrtforschung, Vol. VII, No. 1, April 30, 1930, pp. 43-58. For Parts I and II, see N.A.C.A. Technical Memorandums Nos. 596 and 597.

and quality of the driven rivet alone should be the deciding factor in judging the quality of the rivet material, because its strength characteristics may be changed considerably by riveting. He proves by a series of tests that the yield point and the tearing strength of driven and plain rivets yield decidedly higher values when the rivet material of the driven rivet is examined.

TABLE XXIV

Yield point and tensile strength of driven and plain rivets (mean values).

Condition with identical rivet material	Yield point kg/cm^2	Tensile strength kg/cm^2
Rivet bar	2520	3890
Rivet - plain	4220	4930
Rivet - driven	4020	5030

These figures correspond to about 60% increase in yield point and about 28% increase in tensile strength in the material of the driven as well as the plain rivets in contrast to the corresponding strength values of the rivet bar material. Of course with subsequent annealing those higher strength figures are practically wiped out and the rivet bar material reassumes its original figures. Using these strength figures ameliorated by clinching as basis for the preceding values for the σ_S/σ_Z ratio (for steel St. 37 and St. 48 ~ 0.7 - 0.8), disregarding the increased shearing strength due to riveting, the result

would be lower values for σ_S/σ_Z = ~0.55 - 0.6. But this, moreover, implies that the ratio σ_S/σ_Z can be the same for steel as for duralumin when the strength of the driven rivet material is included in the comparison.

But do these conditions apply to duralumin as well? Is it possible to determine for duralumin an increase in strength characteristics after working the rivet material? As a matter of fact, clinching strengthens the material and through it improves the strength characteristics. In the following we cite the figures of several shear tests on plain and driven duralumin rivets, made in the Junkers and in the Rohrbach shops.

1. To determine the shearing strength of duralumin rivets (alloy 681a) due to working, we applied the same test to single-rivet double shear test specimens with driven and plain heat-treated rivets. Rivet plates and straps were of 2 mm sheet iron to forestall enlargement of the rivet holes. The rivet diameter was 3.0 mm, the hole diameter 3.1 mm (drilled).

TABLE XXV

Shearing strength of plain and driven duralumin rivets

a) rivets, plain-double shear				b) rivets, hand driven double shear			
Ultimate load P kg	Rivet diam. d mm	Rivet cross section f mm²	Shearing strength $\sigma_S = \frac{P}{2.f}$ kg/mm²	P kg	d mm	f mm²	$\sigma_S = \frac{P}{2.f}$ kg/mm²
340 355 330 345	3.0	7.0	↓	400 395 420 440 395 390	3.1	7.5	↓
Average 343.0	3.0	7.0	22.3	Average			27.1

The hand driven rivets showed a 20% higher shearing strength than the plain rivet. Of course, one condition merits special attention. The kind and manner of rivet work during clinching, as in hand riveting, will always depend on the skill of the worker and is subject therefore to variations. Test riveting for experimental purposes always shows satisfactory strength, but in ordinary shop work defects and differences are more apt to occur.

That clinching and working the rivet by hand or machine can produce entirely different strength values is shown in Table XXVI. It is the result of a comparative shear test on single shear, single rivet test specimens, hand and machine driven.

TABLE XXVI

Shearing strength of differently clinched duralumin rivets. Rivet diameter = 3.0 mm; hole diameter = 3.1 mm; rivet cross section : riveted : f = 7.05 mm^2; rivet material : dural : alloy 681a heat-treated; plate material : sheet iron = 2.00 mm. (The plate strips were polished prior to riveting. Specimens tested 5 days later.)

a) Rivets, hand driven, hammer weight 200 g, blows (light) 16 - 18, of which 8 - 9 for clinching.	b) Rivets, machine riveted on eccentric press, maximum pressure 6000 kg, maximum area 160 mm^2 by material strength of 45 kg/mm^2.
Ultimate load P kg	Ultimate load P kg
182.0	238.0
197.0	237.0
187.0	252.0
193.0	223.0
176.0	240.0
185.0	228.0
188.0	234.0
172.0	235.0
192.0	227.0
183.0	209.0
Average 185.5	Average 232.3
$\sigma_s = \frac{P}{7.05} = \boxed{26.3\ kg/mm^2}$	$\sigma_s = \frac{P}{7.05} = \boxed{32.9\ kg/mm^2}$

The rivets driven by the eccentric press show 25% higher shearing strength than those driven by hand, thus proving the marked effect of the better working throughout of the rivet material by the eccentric press. The body of the rivet is clinched better and more evenly than when hand riveted. On the other hand, the material must be more thoroughly and evenly compressed in eccentric press riveting as is evidenced by the necessity of about 1 mm greater body length (10.0 mm against 9.2 mm) than in hand driven rivets.

Basing his statement upon extensive tension tests of duralumin rivets, Prof. Schnadel points to the higher tearing

strength of driven rivets, another proof of the strengthening effect of working the rivet material.

From Brinell hardness tests on cold driven, heat-treated duralumin rivets (alloy 681a) of from 8 - 22 mm diameter, R. Beck determined that the rivet body and especially the rivet head and the second head show some, although not appreciably, greater hardness than stored material due to the strong compression while being worked.

Findeisen likewise states that the shearing strength on riveted joints in iron construction can be essentially higher than that of the rivet material, not only on account of the existing friction, but chiefly on account of the hardening of the rivets when pressing the rivet head and of the clinching when closing.

The discrepancies in working the rivets during clinching and their effect on its strength characteristics after driving make detailed preliminary experiments imperative, if the constructor is to take advantage of this amelioration in strength for the design of structural components which involve riveting. Figure 91 shows such an arrangement. The inserted plates were 1/10 mm thicker than the dural test plates, in order to keep the friction between plate and strap at a minimum. The bolts were of silver steel ($\sigma_B = \sim 330$ kg/mm) surface ground and housed in high tensile steel bushings. The hole diameter was the same for the whole test series: 6 mm;

care was taken that the bolts were always used for one certain hole. To make sure that the holes were smooth and round, they were drilled, one by one, which a 5.9 mm drill and then reamed to 6 mm.

Test Procedure

1. Test series

Dimensions:

e = constant = 15 mm = 2.5 · d, } d = hole diameter
r = constant = 15 mm = 2.5 · d, } = 6.0 mm
s = variable from 0.3 - 3.0 mm.

The first series was used to determine the crushing strength for various plate thicknesses. The effects of the edge distances e parallel and r perpendicular to the tension had to be kept negligibly small (Fig. 92); but since these effects had not been determined numerically, we made e and r = 2.5 · d, and chose equal plate width and equal edge distance for all plate thicknesses s = 0.3, 0.5, 0.8, 1.0, 1.5, 2.0, 2.5 and 3.0 mm. The dimensions in width and thickness near the rivet hole were accurately measured at different points (Fig. 93) and later used for defining the mean value.

A second requirement which permits of no looseness in the rivet joint, due to stresses while in operation, induced us to make elongation measurements on the rivet bolt joints of the s = 0.5, 1.0, 1.5 and 2.0 mm plate specimens with Baumann tensiometers, set on both sides directly behind the bolts over the a - a measuring length (100 mm) of both dural plates

which were to be tested for crushing strength (See Fig. 101). We measured the total and the permanent elongations for the respective load stages by repeated loading and unloading on a 5 ton Mohr and Federhaff testing machine. After exceeding the limit of elongation - about 4/10 mm - of the Baumann tensiometer, we tested them to destruction and measured the elongation on a maximum indicator scale - about 1/10 mm - for the next load stages.

2. Test series

Dimensions:

s = constant = 1.5 mm,
r = constant = 17 mm = about 2.8 d,
e = varying from 0.5 d to 4.5 d = 3.0 to 27.0 mm,

i.e., according to Table XXVII.

TABLE XXVII

Dimensions of test specimens for series II.

e (mm) =	3.0	4.5	6.0	9.0	12.0	15.0	21.0	27.0
=	0.5 d	0.75 d	1.0 d	1.5 d	2.0 d	2.5 d	3.5 d	4.5 d

The second test series merely served to determine the crushing strength by failure for different edge distances e parallel to the pull, Figure 94. As basis we used a constant plate thickness s = 1.5 mm and a constant edge distance e = 17 mm = approximately 2.8 d. We chose plate thickness b because we found after concluding the first test series that no higher crushing strength could be obtained for plates s = 1 mm or over, and that the difference in strength was slight. The

selection of a conical edge distance r, whose effect had not been explained for different r, was made in support of a series of tests made at the München, Karlsruhe and Dresden technical high schools, which showed no appreciable increase in crushing strength for any r greater than r = ~ 3.0 d. For the rest, the dimensions of the set-up, diameter of rivet hole and bolts were the same as in the preceding test series. The elongation tests were eliminated in this and in the next series; the load was applied progressively until rupture.

In this as well as in the subsequent tests we dispensed with clamping two plate specimens into the device at once; one plate of duralumin was used to determine the crushing strength, while the other of steel merely served for clamping in the upper holder of the testing machine.

3. Test series

Dimensions:

s = constant = 1.5 mm,
e = constant = 15 mm = 2.5 d,
r = varying from 0.5 d to 3.5 d = 3.0 to 21.0 mm,

i.e., according to Table XXVIII.

TABLE XXVIII

Dimensions of test specimens for series III

r (mm) =	3.0	4.5	6.0	9.0	12.0	15.0	18.0	21.0
=	0.5 d	0.75 d	1.0 d	1.5 d	2.0 d	2.5 d	3.0 d	3.5 d

Like the second, the third series served to determine the crushing strength by failure plotted against edge distance r

perpendicular to the direction of pull by constant plate thickness s = 1.5 mm and constant edge distance e = 15 mm = 2.5 d (Fig. 95). The third series was tested under the same conditions.

It was already becoming evident in the first and in the second test that the most highly stressed portion of the hole, just before reaching the ultimate stress, suffered strange deformations and thickening at this point and it was feared that the small distances between plates and fish plates would form a support for the thicker compressed part, partly through the fish plate walls and partly through the ensuing strong friction which would falsify the actual crushing strength figures. For that reason we cut out on some specimens the parts of the fish plates which might possibly become a support for the plates, so as to give this thickening of the plate free room. However these precautions were unwarranted, for there was practically no difference in the crushing strength figures.

Test Data

1. Test series

The stress-strain measurements on the bolted joints have been reproduced in Figures 96 to 102. They show the strains plotted against the specific crushing strength for the individual load stages. It will be seen that any direct determination of spreading in the holes is impossible in duralumin from the behavior of the stress-strain curve (no distinct bend) because sudden jumps occur only in the rarest cases, and no approximately determined proportionality exists between stress, elongation and deformation. This checks with the characteristic of the dural-

umin which has no visibly distinct limit of yield or proportionality.

Consequently it was unnecessary to define that condition of the riveted joint as limit of safe stress due to hole edges, at which greater permanent and less regular hole deformations occur, for it is impossible to define one distinct point on the whole stress-strain curve.

TABLE XXIX

Crushing strength by failure σ_{LBr} (in kg/mm²) for various plate thicknesses s (in mm) by e and r = constant. (e = edge distance parallel to strain.) (r = edge distance perpendicular to strain.)

Specimen	Mean plate thickness s mm	Area of hole $f_l = s\ 6.0$ mm²	Crushing strength by failure P_l kg	Crushing strength $\sigma_{LBr} = \frac{P_l}{f_l}$ kg/mm²
26.1; 26.2	0.315	1.89	125.0	66.2
27.1; 27.2	0.310	1.86	120.0	64.5
Average	0.312	--	--	65.4
1.1; 1.2	0.530	3.18	285.0	89.6
2.1; 2.2	0.535	3.21	258.0	80.5
3.1; 3.2	0.535	3.21	279.0	87.0
4.1; 4.2	0.535	3.21	265.0	82.6
Average	0.535	--	--	84.9
28.1; 28.2	0.800	4.80	437.0	91.0
29.1; 29.2	0.780	4.68	404.0	86.3
Average	0.790	--	--	88.6

TABLE XXIX (Cont.)

Specimen	Mean plate thickness s mm	Area of hole $f_l = s\ 6.0$ mm^2	Crushing strength by failure P_l kg	Crushing strength $\sigma_{LBr} = \frac{P_l}{f_l}$ kg/mm^2
6.1; 6.2	1.115	6.70	790.0	118.0
7.1; 7.2	1.110	6.66	830.0	124.5
8.1; 8.2	1.110	6.66	800.0	120.0
9.1; 9.2	1.120	6.72	840.0	125.0
10.1; 10.2	1.110	6.66	830.0	125.0
Average	1.115	--	--	122.5
11.1; 11.2	1.520	9.12	1100.0	121.0
13.1; 13.2	1.515	9.10	1090.0	120.0
14.1; 14.2	1.515	9.10	1090.0	120.0
15.1; 15.2	1.515	9.10	1080.0	119.0
Average	1.520	--	--	120.0
16.1; 16.2	1.920	11.52	1420.0	123.5
18.1; 18.2	1.930	11.60	1370.0	118.0
19.1; 19.2	1.940	11.65	1440.0	123.5
Average	1.930	--	--	121.6
30.1; 30.2	2.480	14.88	1810.0	122.0
31.1; 31.2	2.480	14.88	1675.0	112.0
Average	2.480	--	--	117.0
33.1; 33.2	3.000	18.00	2050.0	114.0
34.1; 34.2	3.000	18.00	2010.0	112.0
Average	3.000	--	--	113.0

These questions will be discussed in a later chapter.

Table XXIX shows the crushing pressure by failure, and the crushing strength σ_{LBr} (in kg/mm^2) by failure, with consideration of the cross section of the hole walls in the initial

state. The result is the averages for σ_{LBr} by different plate thicknesses s, shown in Table XXX.

TABLE XXX

Mean values for crushing strength by failure, relative to plate thickness s.

Plate thickness s	mm	0.313	0.535	0.79	1.115	1.52	1.93	2.48	3.00
	multiple of	0.054	~0.09	0.132	0.188	~0.25	0.32	0.415	0.5
Crushing strength by failure σ_{LBr} (kg/mm^2)		65.4	84.9	88.6	122.5	130.0	121.6	117.0	113.0

For any thickness s < 1.0 mm, all σ_{LBr} values increase with the plate thickness. The maximum σ_{LBr} = 120 kg/mm^2 is reached by s = 1.1 mm (approximately) plate thickness, for thicknesses up to s = 3 mm the σ_{LBr} remained practically the same. The slight variations for a certain plate thickness are due to the fact that the quality of the material is not always the same. The somewhat lower crushing strength of plates of over 2 mm is perhaps due to the fact that heavier plates are not always as evenly rolled as thinner sheets.

The results of these tests are graphed in Figure 103, with the σ_{LBr} plotted against plate thickness s. The spread of the σ_{LBr} values for the lower thicknesses was due to the fact that we used duralumin plates of different hardness (1/3 and 1). The low crushing strength by failure σ_{LBr} in thin plates

below 1 mm is solely due to the fact that by this kind of damping of the plates the local compression strength of the hole walls is greatly reduced by the bulging of the highly stressed plate edges. They appear as well defined wave-like, elliptical bulges on the plate edges, beginning at the edge of the hole and spreading outward. This wavy bulging is a characteristic of the lower plate thicknesses, and disappears afterward in thicknesses of more than 1 mm. Figures 104, a to h, breaks in plates to determine crushing pressure - tensile strength for different plate thicknesses; showing wave-like ridges at hole edges. Directly before breaking these ridges pile up and crumble. In all thicknesses $s \geq 1.0$ mm (d to h) crushing pressure - tensile strength remains nearly constant. The breaks are clean crushing failures; holes continue to enlarge up to failure. Figure 105 shows the failures of some plates of all thicknesses tested, the wave-like bulges of the lower plates being particularly noticeable in Figures 104, a to c. The question of hole deformation preceding failure and the amount of deformation will be discussed later.

2. Test series

Table XXXI shows the crushing pressure by failure and the specific crushing strength by failure σ_{LBr} based upon the nominal cross section of the hole area.

By constant plate thickness s (s = 1.5 mm) and constant edge distance r (r = 17 mm) according to Table XXXII, the mean values for σ_{LBr} by different edge distance e, are:

TABLE XXXI

Crushing strength by failure σ_{LBr} (kg/mm²) for different edge distances e with r and s = constant.

Specimen	Mean plate thickness s mm	Edge distance e mm	Edge distance r mm	Hole surface $f_l = s\,d = 6\,s$ mm²	Crushing pressure by failure P_l kg	Crushing strength $\sigma_{LBr} = \frac{P_l}{6\,s}$ kg/mm²
40	1.52	3.1	16.85	9.12	394	43.2
41	1.52	3.1	17.00	9.12	380	41.6
42	1.51	3.1	17.00	9.06	408	45.0
43	1.525	3.0	16.95	9.15	397	43.4
44	1.52	3.0	16.95	9.12	392	42.9
Average	1.52	3.06	16.95	--	--	43.2
91	1.50	4.4	17.00	9.00	477	52.8
92	1.50	4.5	17.05	9.00	496	55.0
93	1.51	4.4	16.90	9.06	490	54.1
94	1.49	4.4	17.00	8.94	473	52.8
95	1.51	4.5	17.00	9.06	490	54.0
Average	1.50	4.55	17.00	--	--	53.7
45	1.52	6.0	16.80	9.12	--	--
46	1.50	6.0	16.85	9.00	602	66.8
47	1.50	6.0	16.95	9.00	590	65.5
48	1.51	5.9	16.85	9.06	586	64.6
49	1.52	6.0	16.90	9.12	608	66.5
Average	1.51	6.0	16.90	--	--	65.7
50	1.51	8.9	17.20	9.06	790	87.0
51	1.51	8.9	16.95	9.06	797	88.0
52	1.52	8.7	16.90	9.12	778	85.0
53	1.51	9.0	17.00	9.06	796	88.0
54	1.51	8.9	16.95	9.06	808	89.0
Average	1.51	8.9	17.00	--	--	87.4

TABLE XXXI (Cont.)

Specimen	Mean plate thickness s mm	Edge distance e mm	Edge distance r mm	Hole surface $f_l = s\,d = 6\,s$ mm²	Crushing pressure by failure P_l kg	Crushing strength $\sigma_{LBr} = \frac{P_l}{6\,s}$ kg/mm²
55	1.51	12.0	16.95	9.06	947	104.0
56	1.51	11.9	17.00	9.06	954	105.5
57	1.51	11.9	17.00	9.06	951	105.0
58	1.51	12.0	16.90	9.06	953	105.3
59	1.49	11.9	17.00	8.94	931	104.0
Average	1.51	11.95	17.00	--	--	104.8
60	1.52	14.7	17.00	9.12	1054	115.8
61	1.51	14.9	17.05	9.06	1048	116.0
62	1.51	14.7	17.05	9.06	1051	116.3
63	1.51	15.0	17.05	9.06	1070	118.0
64	1.50	14.9	17.05	9.00	1060	117.5
Average	1.51	14.85	17.05	--	--	116.7
65	1.52	21.0	16.95	9.12	1176	129.0
66	1.51	20.9	16.80	9.06	1020	112.8
67	1.51	21.6	16.75	9.06	1043	115.2
68	1.51	20.9	16.80	9.06	1028	113.5
69	1.515	21.1	16.95	9.09	1048	115.7
Average	1.510	21.1	16.85	--	--	117.2
70	1.49	27.0	17.00	8.94	1016	113.6
71	1.49	27.0	17.00	8.94	1041	116.5
72	1.51	27.0	16.80	9.06	1018	112.4
73	1.51	27.0	16.80	9.06	1045	115.3
74	1.50	26.9	17.00	9.09	--	--
Average	1.50	27.0	16.90	--	--	114.5

TABLE XXXII

Mean value of crushing strength by failure relative to edge distance e.

Edge distance	in mm	3.06	4.45	6.0	8.9	11.95	14.85	21.1	27.0
	in multiples of	~0.5	~0.75	1.0	~1.5	~2.0	~2.5	~3.5	4.5
Crushing strength by failure σ_{LBr} kg/mm^2		43.3	53.7	65.7	87.4	104.8	116.7	117.2	114.5

The results of the measurements are shown in graph, Figure 106, with σ_{LBr} plotted against e. The σ_{LBr} curve is almost straight within e = 0.5 - 2.5 d for greater distance of e. Beginning at e = ~ 2.5 d and beyond the curve runs practically parallel to the abscissa, and shows a maximum of σ_{LBr} = about 115 kg/mm^2 for all e. Within $e \geq 2.5$ d it is constant. By smaller edge distance it drops, due to the exhaustion of shearing stress in s e until rupture and shear of respective hole edge.

Figure 107 shows some of the characteristic plate failures for different edge distances. In holes close to the plate edge, (a to e in Fig. 107) the break appears as smooth shearing off, while for these with the hole farther from the edge (g to h in Fig. 107) the break continues as outward cracks, running at 45° to the direction of the tension. In the specimens with hole close to the edge, the bulges around the hole were plainly visible, but not on those with holes farther away from the edges.

If $e \leq 2\ d$ the tensile strength decreases because the shearing stress on $s\ e$ is exhausted. If $e > 2\ d$ specimens show usual breaks, the tensile strength of the plates is nearly constant.

a) Edge distance e = 3.0 mm = 0.5 d
b) Edge distance e = 4.5 mm = 0.75 d
c) Edge distance e = 6.0 mm = 1.0 d
d) Edge distance e = 9.0 mm = 1.5 d
e) Edge distance e = 12.0 mm = 2.0 d
f) Edge distance e = 21.0 mm = 2.5 d
g) Edge distance e = 21.0 mm = 3.5 d
h) Edge distance e = 27.0 mm = 4.5 d

In plates with $e < 2.0\ d$, the break occurred as smooth shearing off of the part below the bolt. However, it would be misleading to speak here of exhaustion of the crushing strength, due to failure of the bearing capacity of the hole walls. The plate section under crushing stress P, is in addition stressed in shear in section $(s\ e')$, which in all cases where $e < 2\ d$, is perhaps the deciding factor of the plate strength (Fig. 108). For this shear stress $\sigma_{S'Br} = \frac{P_{Br}}{2\ e'\ s}$ (kg/mm²), the equation $P_{Br} = 2\ e'\ s\ \sigma_{S'Br}$ is valid. While in machine construction e' is generally $(e + d/2)$, we use $e' = (e + d/4) = (e + 1.5\ mm)$. According to Table XXXIII, we now have:

TABLE XXXIII

Shearing strength of hole edge zone in direction of tearing.

Specimen (See table 32.)	Plate thickness s mm	Edge e' mm	s e' mm^2	Ultimate load P_{Br} kg	$P_{Br}/2$ kg	Shearing strength by failure $\sigma_{S'Br}$ kg/mm^2
40	1.52	4.6	6.992	394	197	28.2
93	1.51	5.9	8.91	490	245	27.5
47	1.50	7.5	11.25	590	295	26.2
49	1.52	7.5	11.40	608	304	26.6
51	1.51	10.4	15.70	797	398.5	25.5
54	1.51	10.4	15.70	808	404	25.7

The calculated $\sigma_{S'Br}$ values agree with the values of the shear strength σ_{SBr} of duralumin rivets (σ_{SBr} = 26-28 kg/mm^2) and substantiate the above assumption that the shearing stress in the cross section area (s.e') by $e < 2.0\ d$ is always exhausted to failure under the present stresses.

TABLE XXXIV

Crushing strength by failure σ_{LBr} kg/mm² for various edge distances, r perpendicular to the direction of pull, with e and s = constant.

Specimen	Mean plate thickness s mm	Edge e mm	Edge r mm	Hole area $f_l = 6.0 \cdot s$ mm²	Crushing by failure P_l kg	Crushing strength by failure = $\frac{P_l}{f_l}$ kg/mm²
75	1.51	15.0	3.00	9.06	392	43.2
75 a	1.515	15.1	3.00	9.09	384	42.2
76	1.51	14.9	3.00	9.06	378	41.8
76 a	1.515	15.1	3.00	9.09	386	42.4
77	1.50	15.0	3.00	9.00	369	41.0
77 a	1.505	14.9	3.00	9.03	373	41.3
78	1.50	14.9	3.00	9.00	383	42.6
78 a	1.515	15.1	3.00	9.09	395	43.5
79	1.50	14.8	3.00	9.00	377	41.8
Average	1.508	15.0	3.00	--	--	42.4
80	1.50	15.0	4.50	9.00	568	63.0
81	1.51	15.0	4.50	9.06	570	63.0
81 a	1.52	15.0	4.50	9.12	561	61.6
82	1.51	15.2	4.50	9.06	568	62.7
82 a	1.52	15.1	4.50	9.12	561	61.6
83	1.51	15.1	4.50	9.06	570	63.0
83 a	1.515	15.0	4.50	9.09	570	62.5
84	1.51	14.9	4.50	9.06	565	62.4
Average	1.51	15.05	4.50	--	--	62.4
86	1.51	15.1	6.00	9.06	780	86.0
86 a	1.525	15.0	6.00	9.15	741	81.0
87	1.51	14.9	5.95	9.06	741	81.8
87 a	1.52	15.2	5.90	9.12	733	80.4
88	1.51	15.0	6.00	9.06	742	81.8
88 a	1.525	15.0	6.00	9.15	747	81.5
89	1.49	15.2	6.00	8.94	737	82.3
90	1.51	15.2	6.00	9.06	747	82.5
Average	1.515	15.1	6.00	--	--	82.0

TABLE XXXIV (Cont.)

Specimen	Mean plate thick-ness s mm	Edge e mm	Edge r mm	Hole area f_l= 6.0 s mm^2	Crushing by failure P_l kg	Crushing strength by failure = $\frac{P_l}{f_l}$ kg/mm^2
101	1.50	14.8	9.00	9.00	943	104.8
101 a	1.52	15.1	9.00	9.12	961	105.2
102	1.50	14.9	9.00	9.00	970/982	109.1
102 a	1.52	15.0	9.00	9.12	934	102.3
103	1.50	15.0	9.00	9.00	965	107.2
103 a	1.52	15.0	9.00	9.12	940	103.0
119	1.50	15.0	9.00	9.00	903	100.3
120	1.50	15.0	9.00	9.00	892	99.1
Average	1.510	15.0	9.00	--	--	103.5
104	1.50	15.1	12.00	9.00	1006	111.2
105	1.50	15.1	11.95	9.00	1009	111.2
106	1.51	15.0	12.00	9.06	996	100.7
106 a	1.52	15.0	12.00	9.12	992	108.8
107	1.51	14.9	12.05	9.06	991	110.1
107 a	1.53	15.0	11.95	9.18	992	108.1
108	1.51	15.1	12.00	9.06	990	110.0
108 a	1.525	15.0	11.95	9.15	1021	111.5
Average	1.51	15.0	12.00	--	--	110.0
96	1.51	15.1	14.90	9.06	995	109.6
97	1.52	15.2	15.00	9.12	987	108.0
98	1.51	15.2	15.00	9.06	981	108.0
99	1.51	15.0	14.90	9.06	986	109.0
100	1.51	15.0	14.90	9.06	1017	112.5
Average	1.51	15.0	14.95	--	--	109.4
109	1.51	15.0	17.90	9.06	947	104.5
110	1.51	14.9	17.80	9.06	1038	114.5
111	1.50	15.0	18.00	9.00	910	100.5
112	1.51	15.1	18.00	9.06	922	102.0
113	1.50	15.0	18.00	9.00	904	100.5
Average	1.51	15.0	18.00	--	--	104.4

TABLE XXXIV (Cont.)

Specimen	Mean plate thickness s mm	Edge e mm	Edge r mm	Hole area f_l = 6.0 s mm^2	Crushing by failure P_l kg	Crushing strength by failure = $\frac{P_l}{f_l}$ kg/mm^2
114	1.50	15.1	20.95	9.00	953	105.9
115	1.49	15.0	20.90	8.94	940	105.0
116	1.49	15.0	20.95	8.94	885	98.6
117	1.50	15.0	20.95	9.00	890	98.8
118	1.49	15.1	21.00	8.94	879	98.2
Average	1.495	15.1	20.95	--	--	101.3

3. Test series

From the crushing pressure by failure, the specific crushing strength at failure σ_{LBr} has been computed for the nominal hole cross section (Table 35). From the selected dimensions and constant plate thickness s(s = 1.5 mm) and edge distance e(e = 2.5 d = 15 mm) depending on the different r (according to Table 35) the following mean crushing strength by failure σ_{LBr} was determined.

TABLE XXXV

Mean crushing strength by failure relative to r.

Edge distance r	in mm	3.0	4.5	6.0	9.0	12.0	15.0	18.0	21.0
	in multiples of	0.5	0.75	1.0	1.5	2.0	2.5	3.0	3.5
Crushing strength by failure σ_{LBr} kg/mm^2		42.2	62.4	82.0	103.5	110.0	109.4	104.4	101.3

The results are shown in Figure 109 with the σ_{LBr} values plotted against r. As in Figure 106, they increase with increasing r within r = 0.5 – 2.0 d; beginning at $r \geq 2.0$ d the crushing strength practically remains the same, the maximum is reached at about $\sigma_{LBr} = 110$ kg/mm².

The drop in the curve for e = 3.0 d and over, is certainly caused only by the different qualities in the materials. Figure 110 shows the breaks on different specimens for different edge distances r as comparison. In this series the break for e (e < 1.5 d) occurred as a tear in height of the rivet hole, i.e., on the weakest cross section stressed in tension, so that the tearing strength of this cross section and not the crushing strength of the hole wall is the deciding factor for all small edge distances r.

For the tearing stress of this cross section (Fig. 111) (b – d) s the following formula is valid:

$$P = (b-d)\,\sigma_Z = 2\,r\,s\,\sigma_Z = \frac{P}{2\,r\,s}\ (kg/mm^2)$$

TABLE XXXVI

Tearing strength of plate section weakened by rivet hole.

Specimen	Plate thickness s mm	Edge distance r mm	2 r mm	2 r s mm²	Ultimate load P_{Br} kg	Tearing strength by failure σ_{ZBr} kg/mm²
75 a	1.515	3.0	6.0	9.09	384	42.2
78 a	1.515	3.0	6.0	9.09	395	43.4
82 a	1.52	4.5	9.0	13.68	561	41.0
83 a	1.52	4.5	9.0	13.68	570	41.6
87 a	1.52	5.9	11.8	17.94	735	40.8
88 a	1.53	6.0	12.0	17.36	747	43.0

The calculated σ_{ZBr} agree very closely with the σ_{ZBr} values (σ_{ZBr} = 41.5 - 42.5 kg/mm^2) for the duralumin plates (alloy 681 B 1/3) and affirm the statement that the tensile strength of the cross section weakened by the rivet hole is already exhausted before reaching the safe crushing strength. Beyond the zone of elastic deformation, the previously uneven stress distribution over the cross section is completely balanced up to the appearance of the break, so that the stress may be assumed as uniformly distributed over the whole cross section, as is borne out by the magnitude of the σ_{ZBr} values.

Föppl, in his "Drang und Zwang," Vol. 1, p. 318, already referred to this apparent paradox, but there is nothing to contradict the facts given here, because in our case it is simply a matter of permanent form changes, while Preuss' experiments dealt with elastic form changes which are governed by Hooke's law.

Th. Wyss* likewise points to the possibility of almost complete stress compensation of a drilled tension plate along the narrowest cross section weakened by a rivet hole, and he also uses Preuss' and Heyman's experiments for comparison. Wyss elucidates this behavior on a fish plate head stressed by a rivet shank.

In the cross section r - r (Fig. 112) there is a possibility of progressing stress compensation under higher

*Th. Wyss, "Die Kraftlinien in festen elastischen Körpern," Verlag Julius Springer, Berlin 1926.

stresses. Within the limit of elastic deformation, the normal stress distribution for r - r and o - o is as shown in Figure 113, (tests of Rühl and Coker*). Type and amount of the normal stress distribution hinges notably on the dimensions of $\frac{c - d}{2}$ and $b - \frac{d}{2}$ (Fig. 113). So, for example, the stress distribution for r - r and o - o is much more favorable when $\frac{c - d}{2}$ and $b - \frac{d}{2}$ are of larger dimensions. After exceeding the yield point by small d and large $\frac{c - d}{2}$, for instance, the tension lines are not quite as strongly forced to tear outward.

Moreover, with the slight bunching of the lines of force and the small stress increases aside from the correspondingly high stresses at the hole edge, the lines of force and the stresses show a steady tendency to compensate. As a result the stress distribution (Fig. 113) of section r - r becomes more and more rectangular (see dotted line).

For cross section o - o we find at larger $(b - \frac{d}{2})$ that the funicular stress curves can tear toward the upper edge, and accordingly, advance toward the outer side walls. This likewise results in a more favorable stress distribution for this section. By small $b - \frac{d}{2}$ (= 14 mm) (Figs. 114 and 115, edge section o - o), the tension stresses are enormous in the center (when approaching the yield point), while the corners show a compression zone. By large $b - \frac{d}{2}$ (= 40 mm) (Figs. 114 and 115, edge section N - N), the stresses at the upper edge are pure tension, which vanish

*E. G. Coker, "The distribution of stress due to a rivet in a plate." Engineering 1913. I, p. 440.

toward the corners.

With regard to the extent of the locally restrained compression zone at the plate edge, due to locally confined compression stresses (See Fig. 112), Wyss points to Rühl's experiments and states that the range of this zone, (called "compression core" by Wyss, and "compression wedge" by Gehler,) depends on the intensity of the existing crushing pressure. Thus, all tension lines intersecting this compression wedge (See Fig. 116) show a part which is under compression. Wyss remarked that the conception of funicular effect is no longer justified for these internal lines of force intersecting the zone of compression. The indirect tension effect, caused by the funicular lines, has a marked influence on the size of the enlargement in the compression zone.

Enlargement of Rivet Holes

One outstanding fact of all our tests is the enlarged holes by failure, which we measured up to 1/10 mm accuracy in the direction of the stress. The enlargement amounted to approximately 1.0 - 4.0 mm, or from 15 to 70% of the original hole diameter d (= 6.0 mm). This applies to specimens loaded to destruction and which showed slight tears, as well as those which failed to show any signs of tearing when stressed only to the first load decrease. These figures have been compiled in Table XXXVII and are for the specimens of the first test series. (See also Figs. 104, 105.)

TABLE XXXVII

Enlargement of rivet holes at beginning of break.

Plate thickness s mm	Original hole diameter d mm	Enlargement Δd	
		mm	% d
0.3	6.1	4.0	65.5
	6.0	4.1	68.5
0.5	6.0	1.8	30.0
	6.0	2.7	45.0
0.8	6.0	3.5	58.5
1.0	6.1	2.7	44.0
	6.0	3.5	58.5
	6.1	3.9	64.0
	6.1	3.4	56.0
	6.1	3.2	52.0
1.5	6.1	3.1	50.5
	6.2	3.9	63.0
	6.3	3.8	60.0
	6.1	3.6	59.0
2.0	6.2	3.4	55.0
	6.2	1.4	22.5
	6.1	2.7	44.5
	6.2	2.8	45.0
	6.1	3.3	54.0
	6.2	1.8	29.0
2.5	6.2	3.2	51.5
	6.1	2.3	28.0
	6.1	1.4	23.0
3.0	6.2	2.4	38.5
	6.2	2.7	43.5
4.0	6.1	1.5	24.5
	6.2	1.7	27.5
	6.1	0.9	15.0
	6.1	0.8	13.0
	6.2	1.3	21.0

The values for the second and third test series were about the same as in the above table for s = 1.5 mm plate thicknesses. Perpendicular to the direction of the stress the original hole diameter is slightly reduced, as we noted when trying to remove the wedged-in bolts.

Another surprise was the pronounced deformation and thickening of the hole walls below the hole edge most heavily stressed by the body of the rivet. It appears in the form of a bulge or ridge, (Fig. 117) which is particularly pronounced at the hole edge and tapers off toward the sides. This bulge increases the cross section of the hole area materially and consequently lowers the specific crushing pressure. Although this cross-sectional enlargement is not to be considered theoretically, it nevertheless should prove of interest to define the amount of maximum bulge w by failure for the different plate thicknesses s. (See 1. test series and table 38.)

TABLE XXXVIII

Thickness of bulge

Plate thickness s (mm)	0.3	0.5	0.8	1.0	1.5	2.0	2.5	3.0	4.0
Thickness of bulge w (mm)	0.85	1.05	1.85	1.75	2.40	2.85	4.0	4.5	5.0

Translation by J. Vanier,
National Advisory Committee
for Aeronautics.

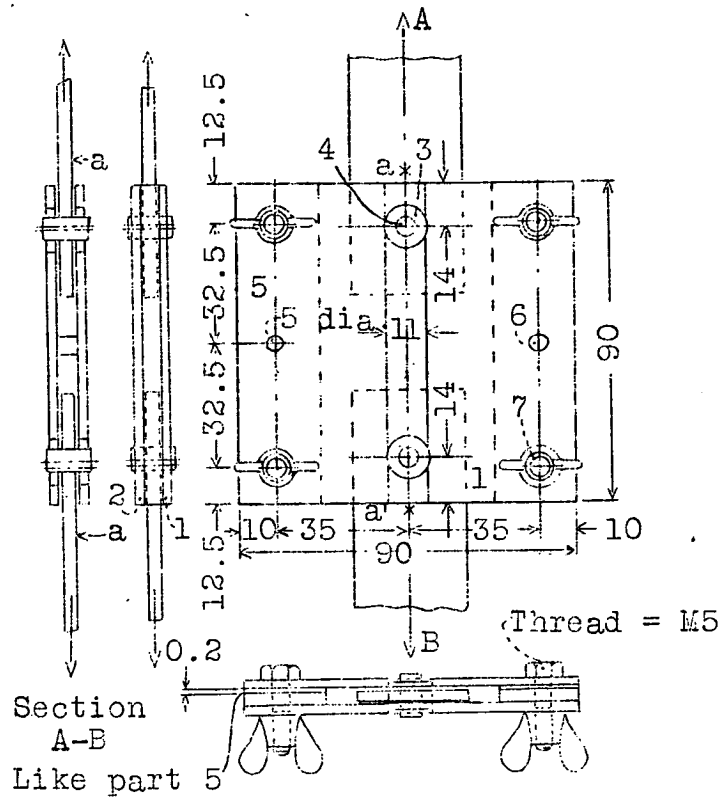

Fig.91 Bolt arrangement for testing crushing strength of plates.

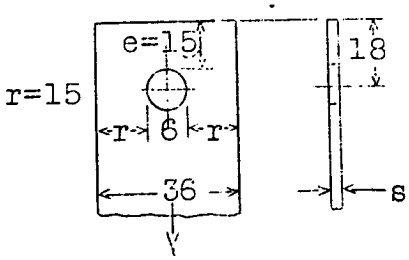

Direction of stress

Fig.92 Size of plate.(I series)

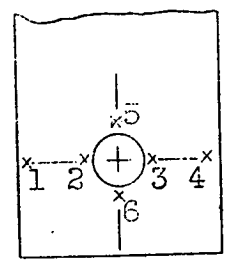

× Point of measurement.

Fig.93 Ridge measurement near hole.

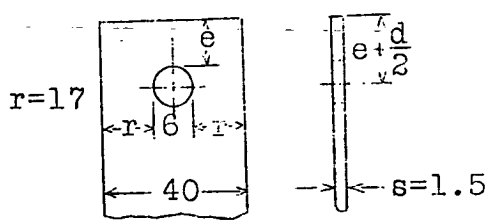

Fig.94 Size of plate,(2 series)

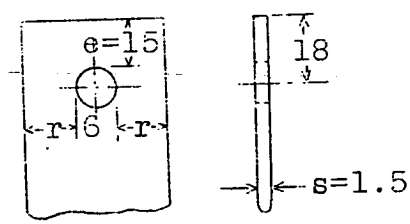

Fig.95 Size of plate. (3 series)

Figs.96-102 Elongation δ plotted against crushing pressure. Curves show no distinct bend. No expressed beginning of break down in hole. Characteristic of duralumin.

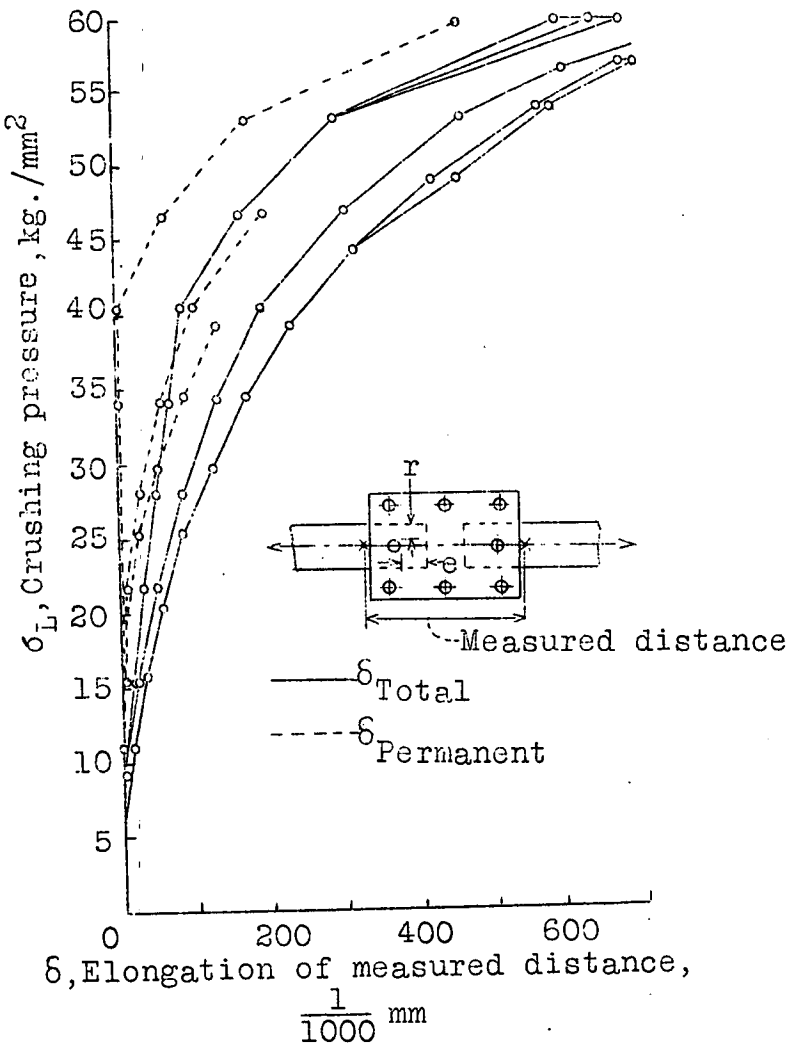

Fig.96 Plate thickness, s=~0.5mm=0.083 d
Edge distance , e= 15.0 mm=2.5 d
" " , r= 15.0 mm=2.5 d

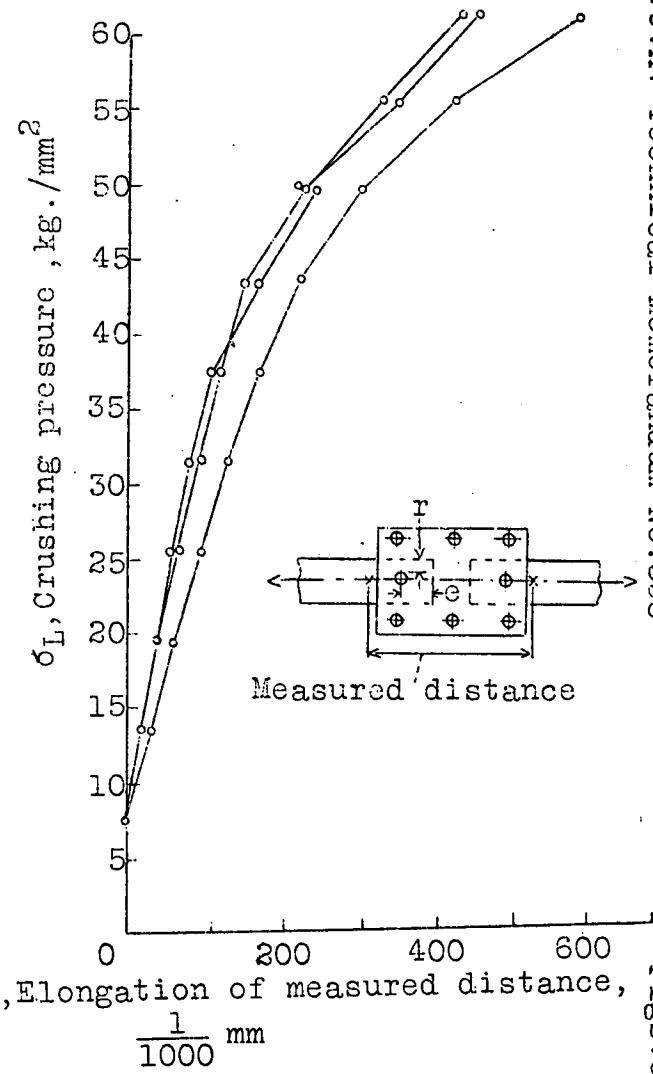

Fig.97 Plate thickness, s=~1.1 mm=0.183 d
Edge distance , e= 15.0 mm=2.5d
" " , r= 15.0 mm=2.5d

Figs.96,97

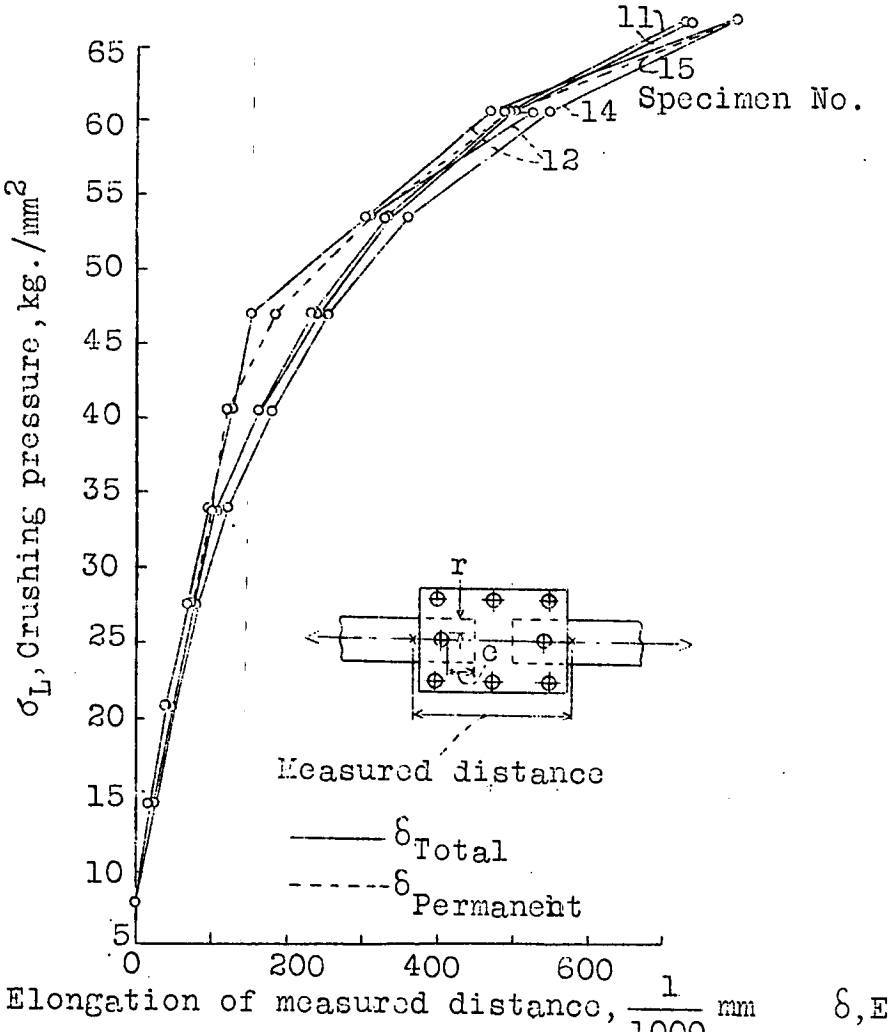

Fig.98 Plate thickness, s=~1.5 mm=0.25 d
Edge distance , e= 15.0 mm=2.5 d
" " , r= 15.0 mm=2.5 d

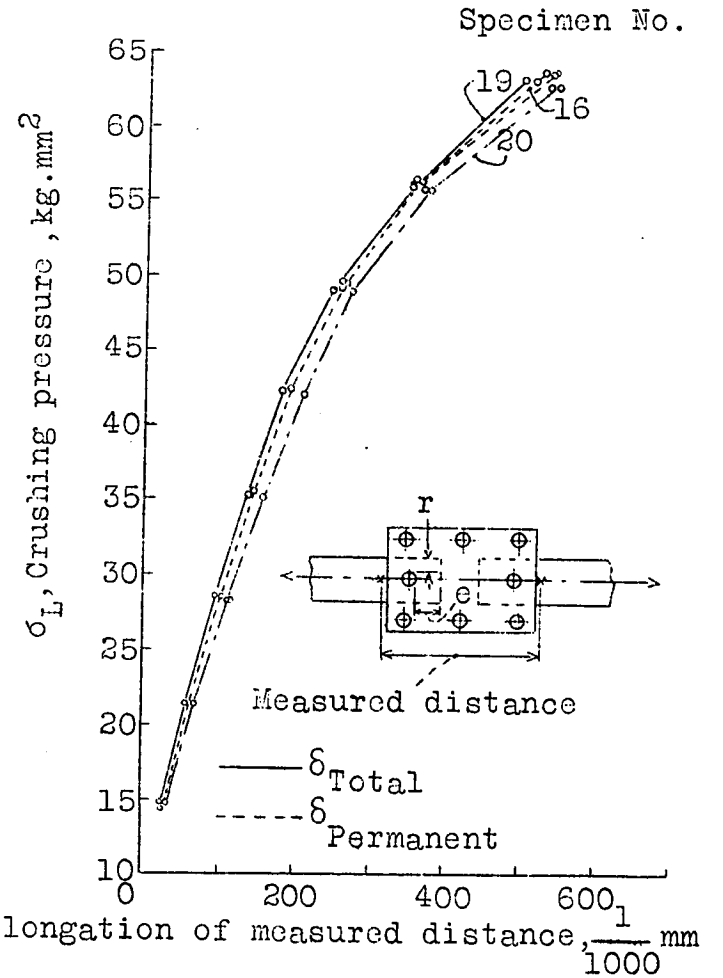

Fig.99 Plate thickness, s=~1.9 mm=0.316 d
Edge distance , e= 15.0 mm=2.5 d
" " , r= 15.0 mm=2.5 d

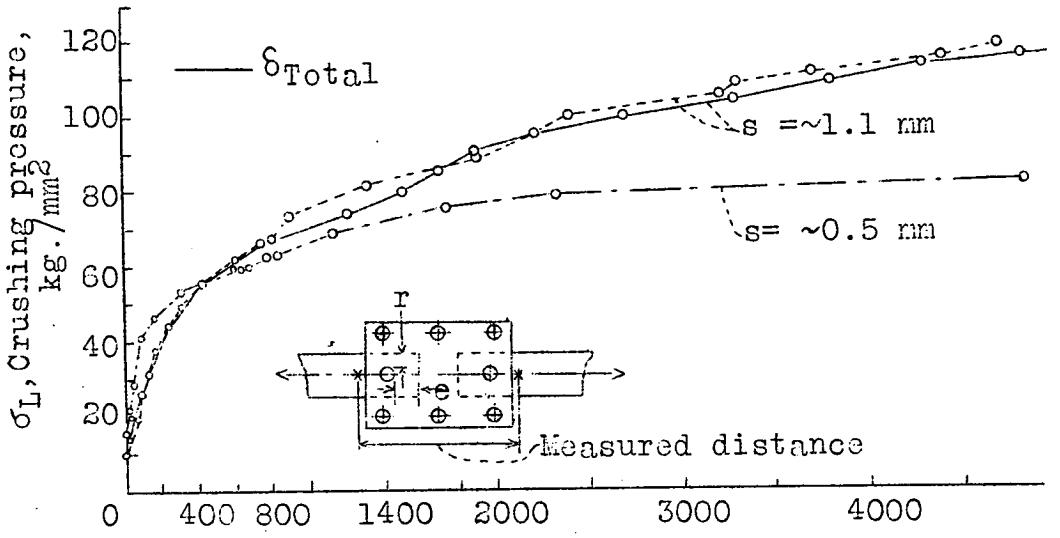

Fig.100 Plate thickness, s=~0.5 mm=0.083 d
" " , s=~1.1 mm=0.183 d
Edge distance , e= 15.0 mm=2.5 d
" " , r= 15.0 mm=2.5 d

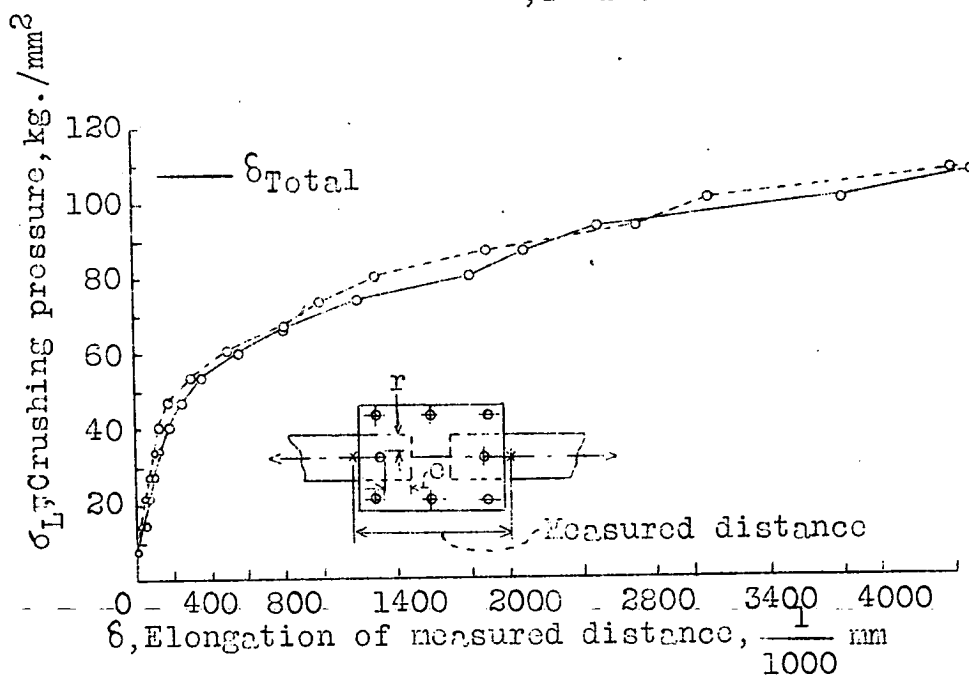

Fig.101 Plate thickness, s=~1.5 mm=0.25 d
Edge distance , e= 15.0 mm=2.5 d
" " , r= 15.0 mm=2.5 d

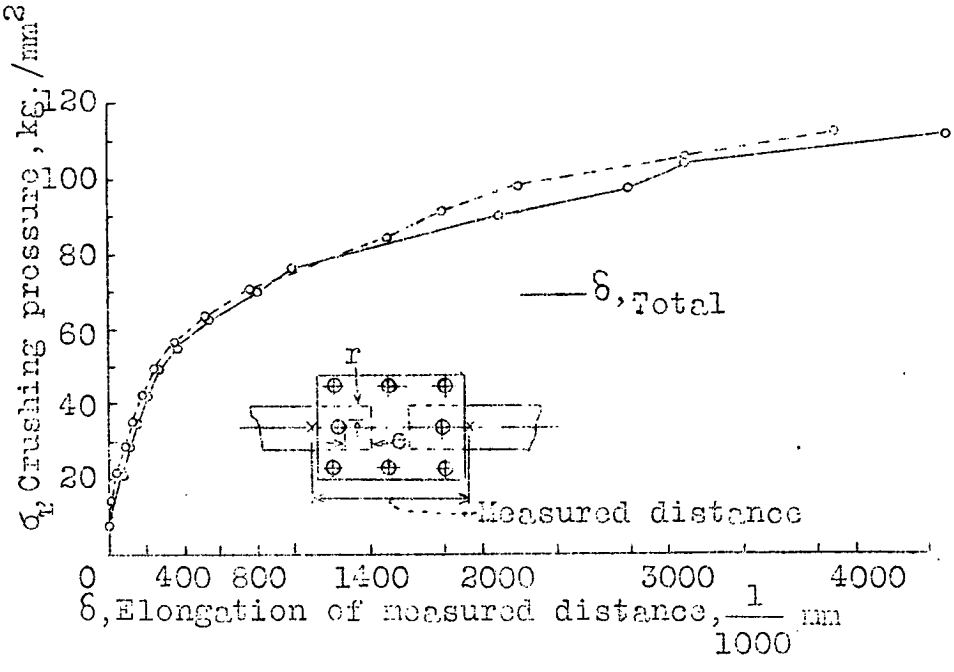

Fig.102 Plate thickness, s= ~1.9 mm=0.316 d
Edge distance , e= 15.0 mm=2.5 d
" " , r= 15.0 mm=2.5 d

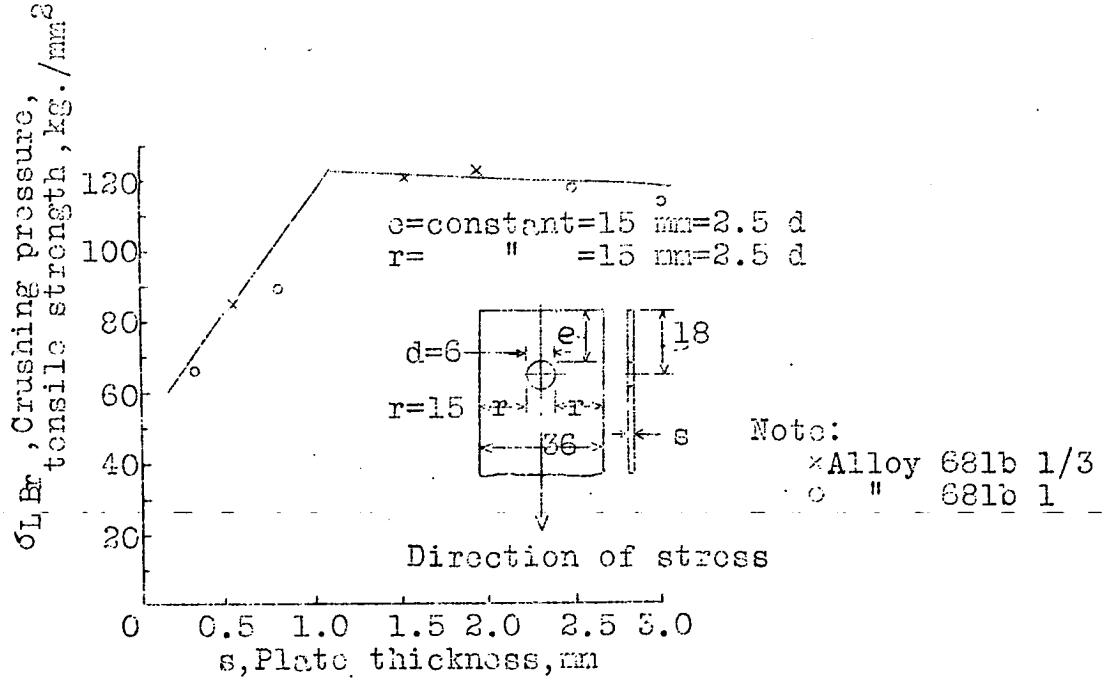

Fig.103 Crushing pressure, tensile strength plotted against plate thickness is nearly constant in a wide range but drops in thin plates due to buckling of hole edge.

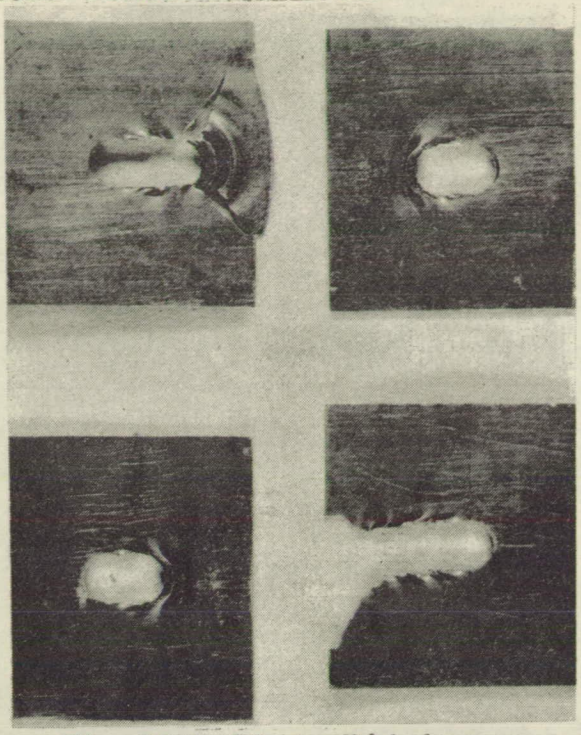

Fig.104a Plate thickness,
s=0.3 mm

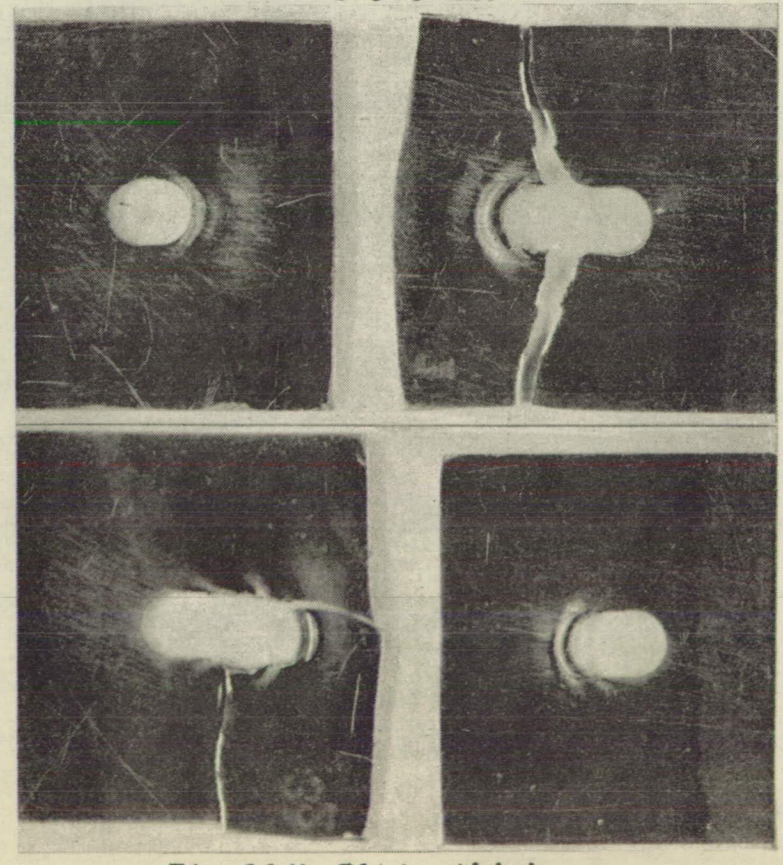

Fig.104b Plate thickness,
s=0.4 mm

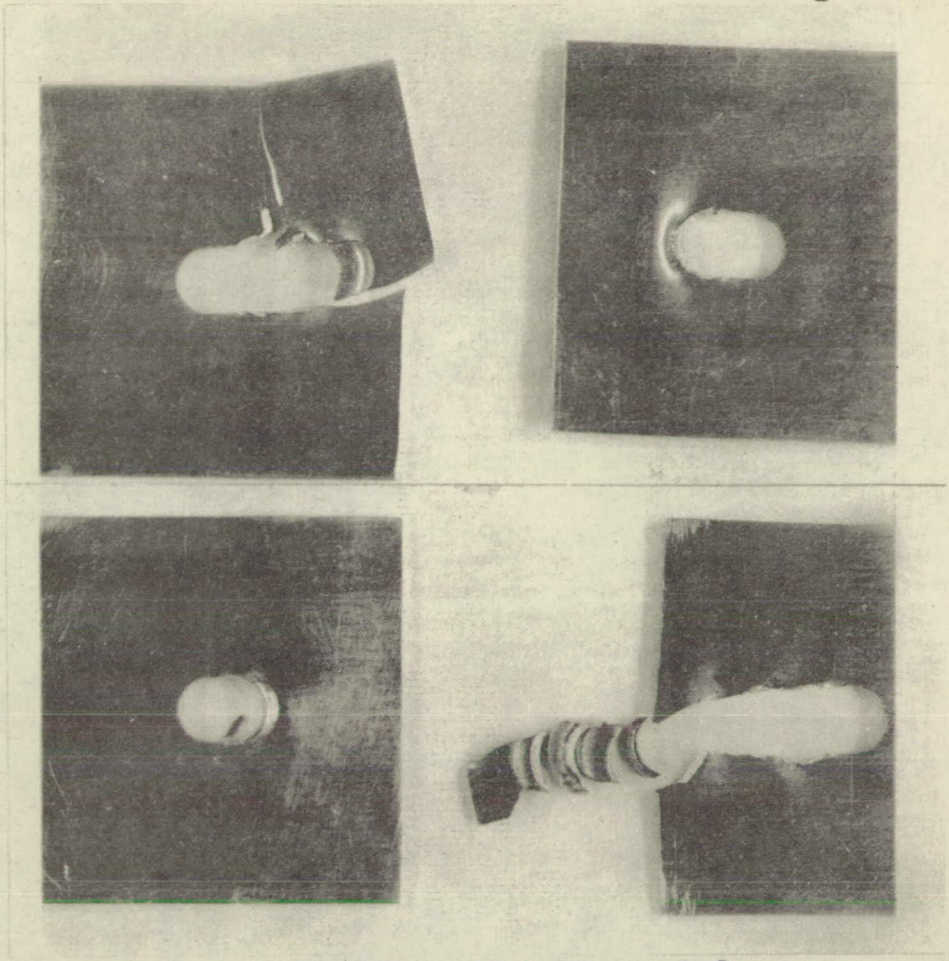

Fig.104c Plate thickness, s=0.8 mm

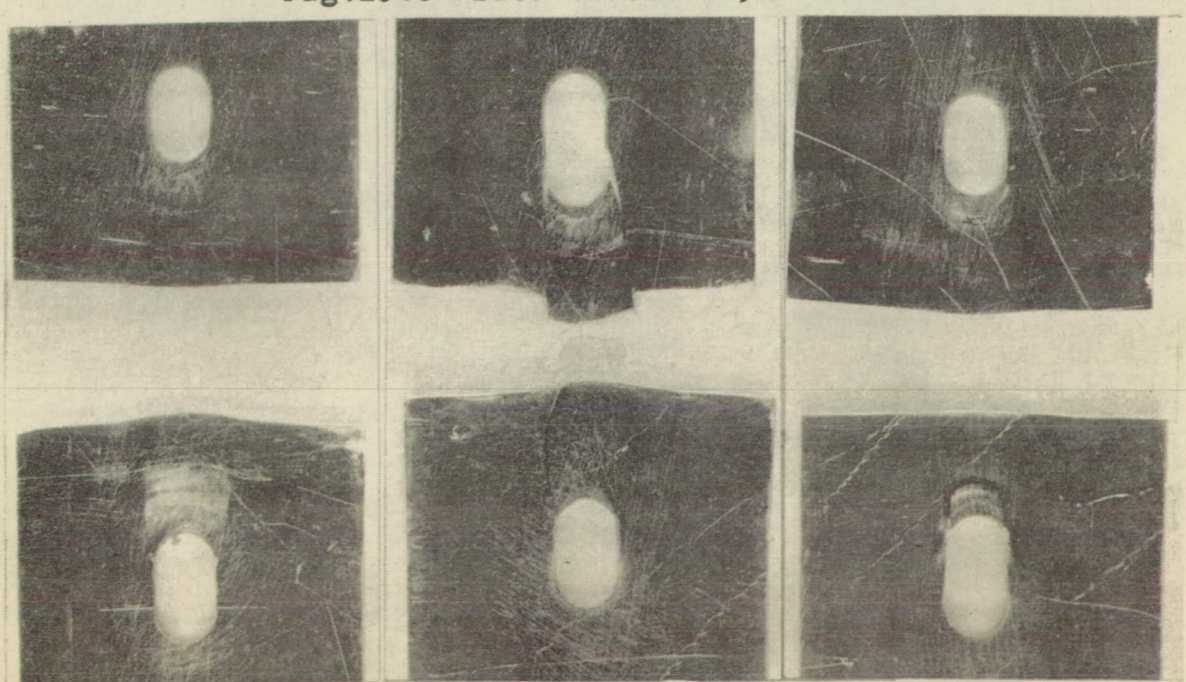

Fig.104d Plate thickness, s=1.0 mm

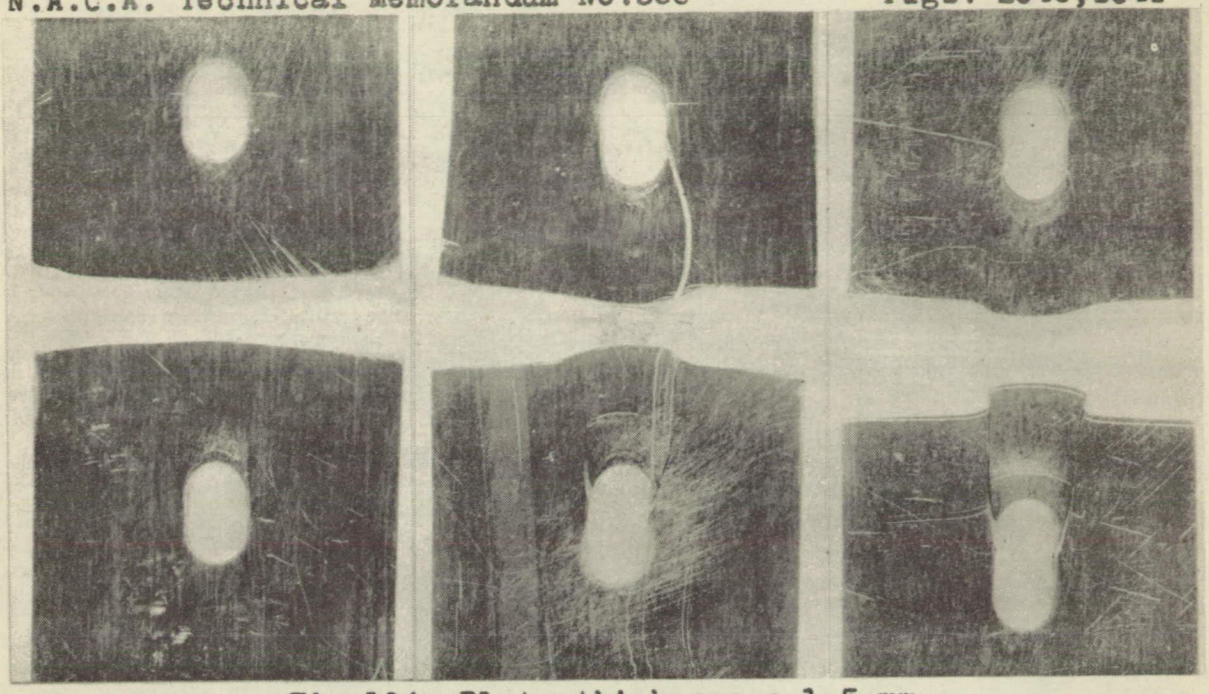

Fig.104e Plate thickness, s=1.5 mm

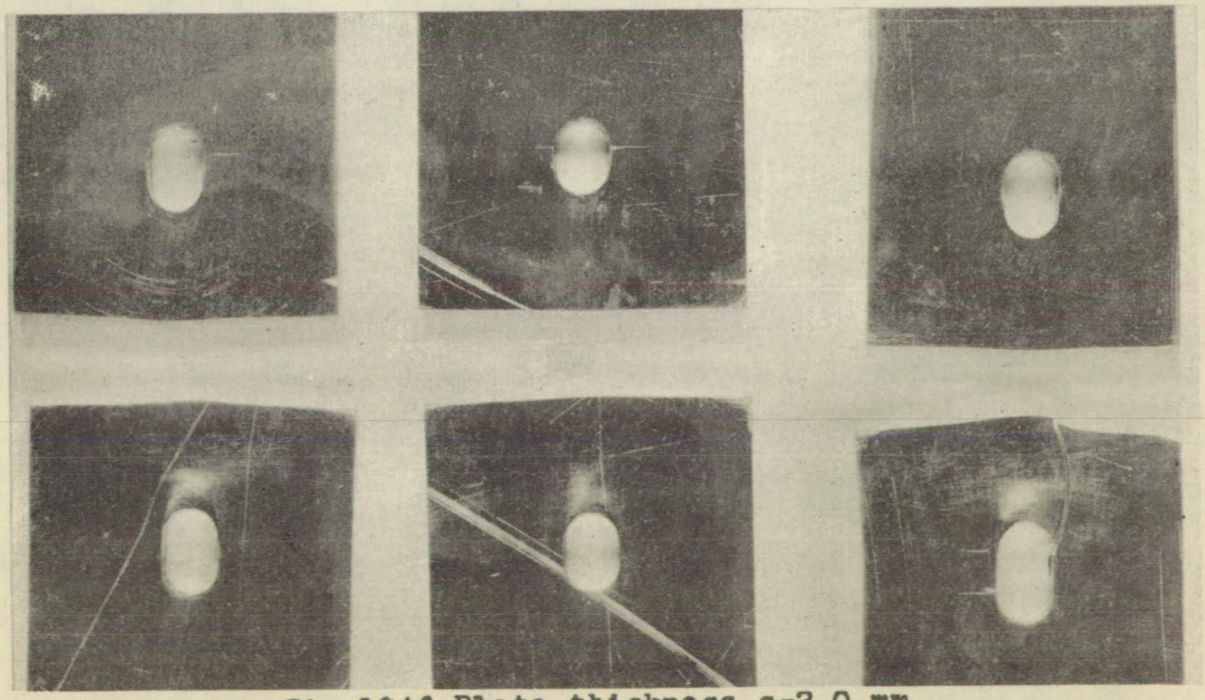

Fig.104f Plate thickness, s=2.0 mm

Fig.104g Plate thickness, s=2.6 mm

Fig.104h Plate thickness, s=3.0 mm

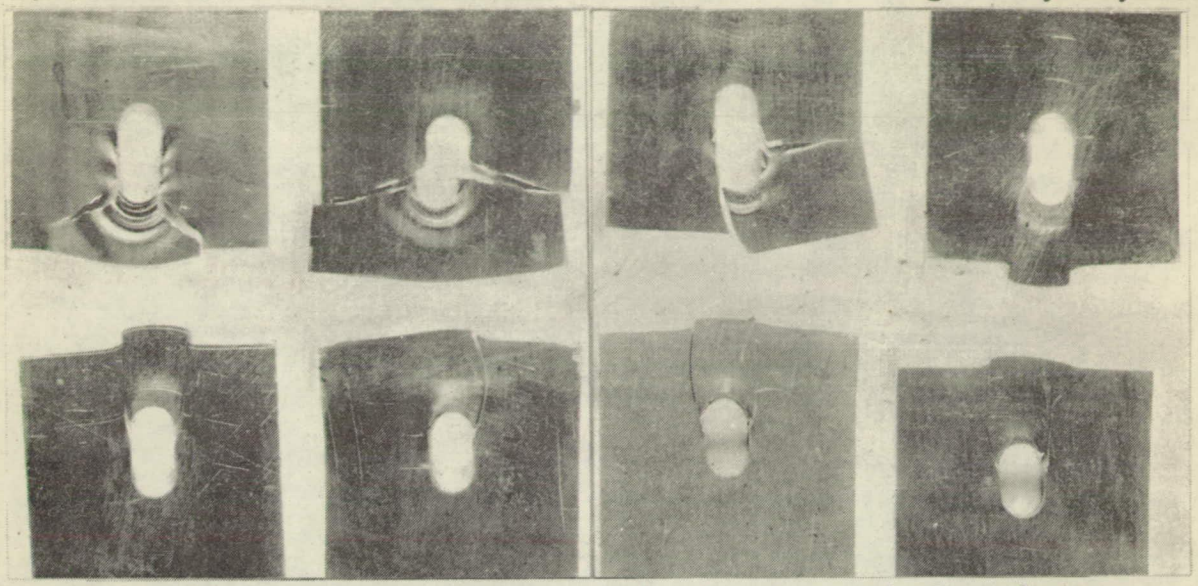

Fig.105 Crushing pressure-ultimate strength for plate thickness s.Top row s=0.3;0.5;0.8;1.0 mm
Bottom row s=1.5;2.0;2.5;3.0 mm

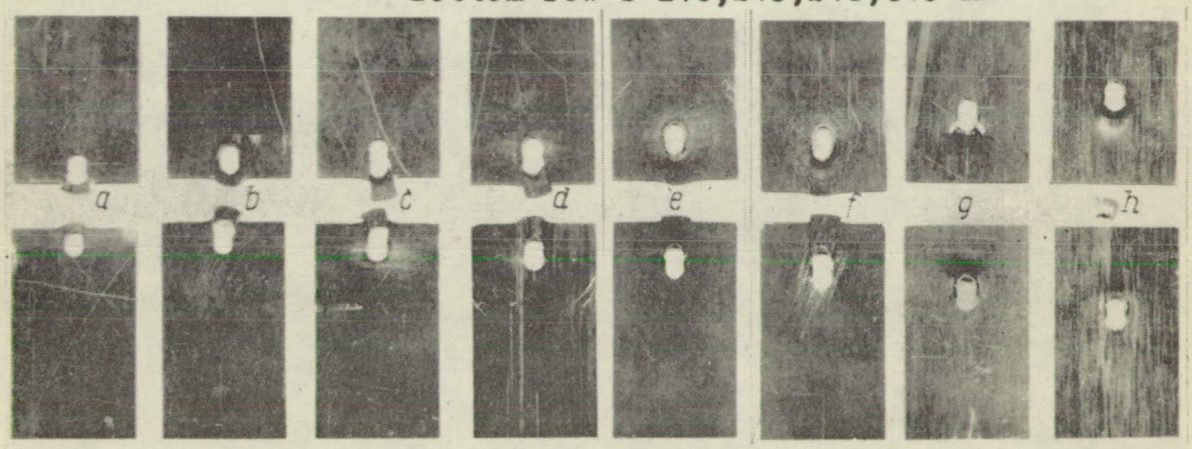

Fig.107 Patterns showing crushing pressure-tensile strength for various edge distances in direction of stress.

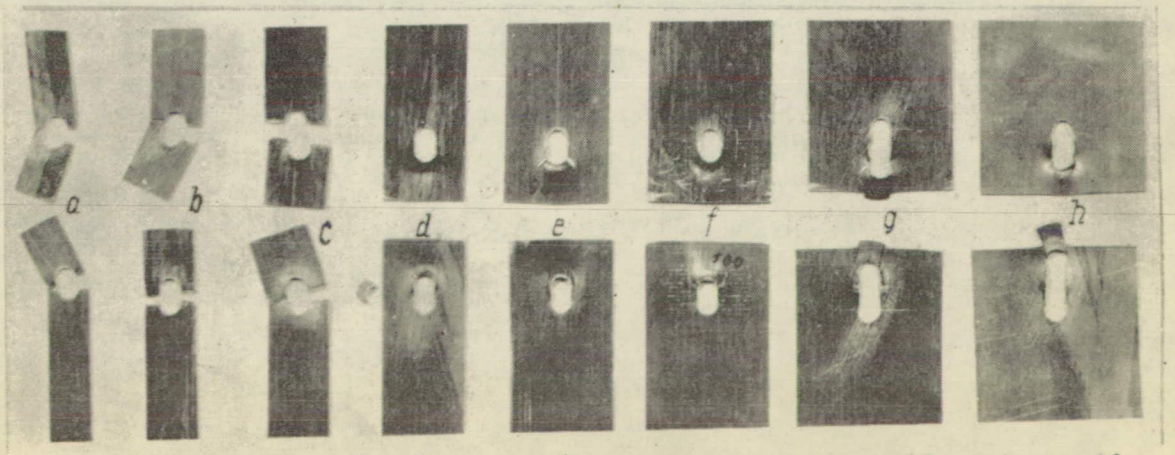

Fig.110 Breaks showing crushing pressure-tensile strength for r perpendicular to direction of stress.

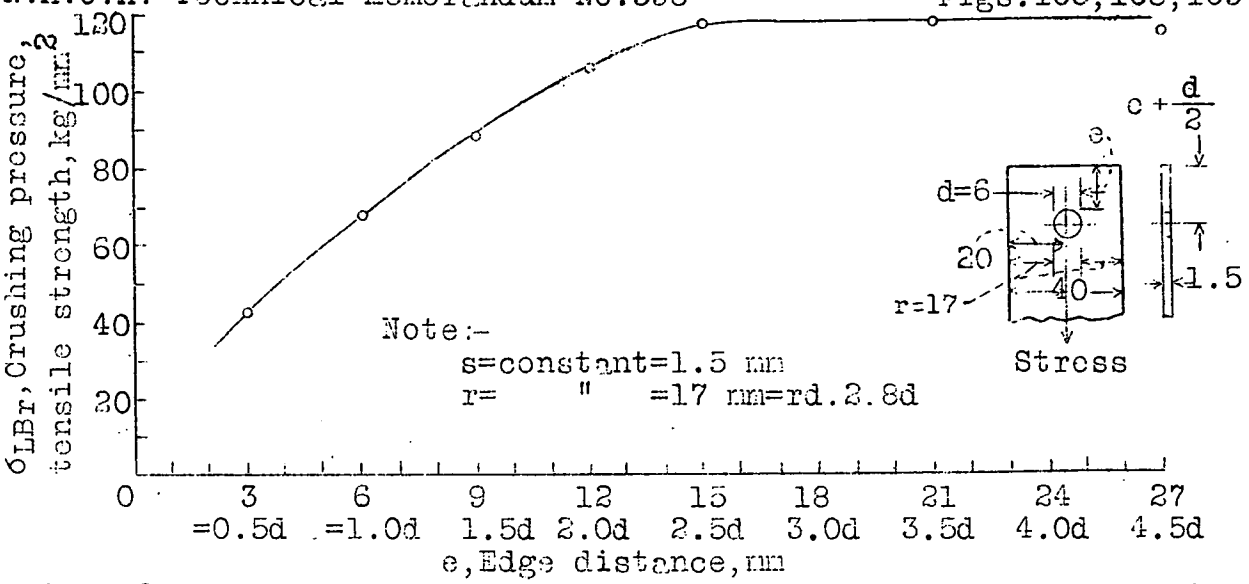

Fig,106 Crushing pressure-tensile strength plotted against e in direction of stress.

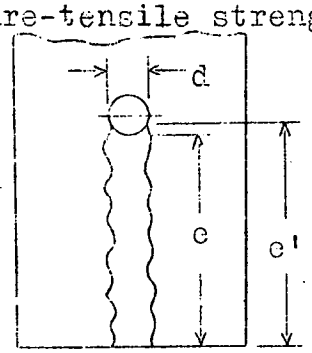

Fig.108 Shearing stress of edge zone of plates.

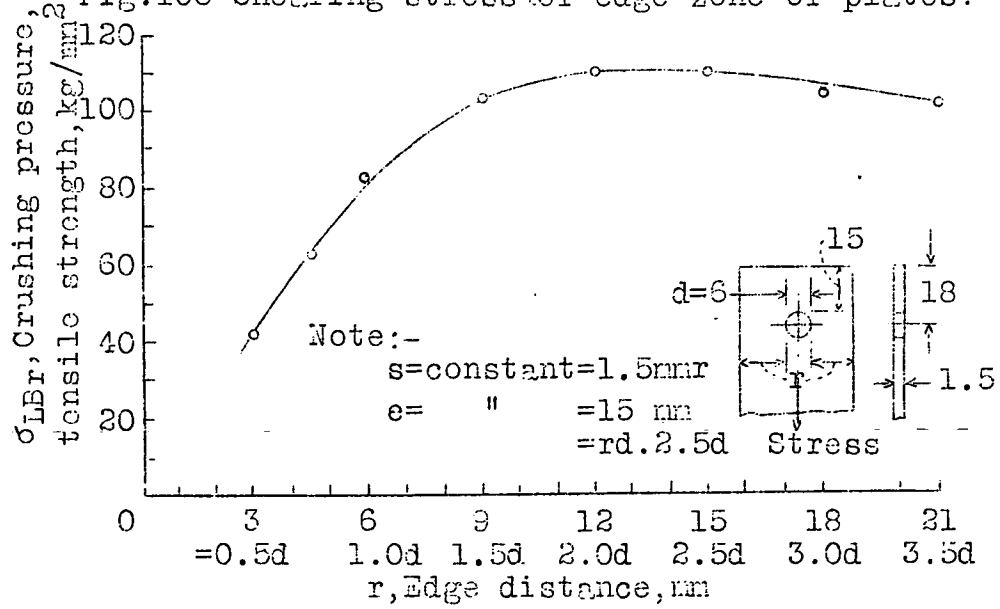

Fig.109 Crushing pressure-tensile strength plotted against r perpendicular to direction of stress.

Figs. 111, 112, 113, 114, 115, 116, 117

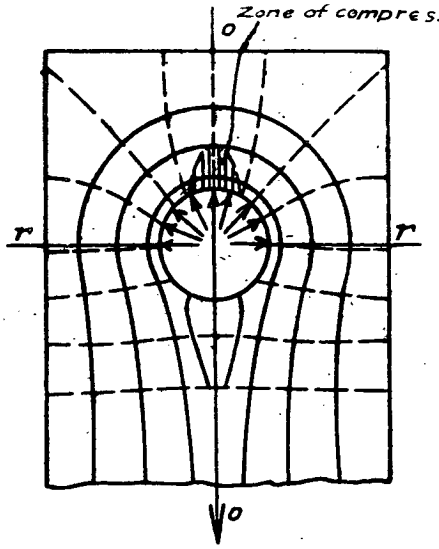

Fig.112 Lines of force in a strap end.

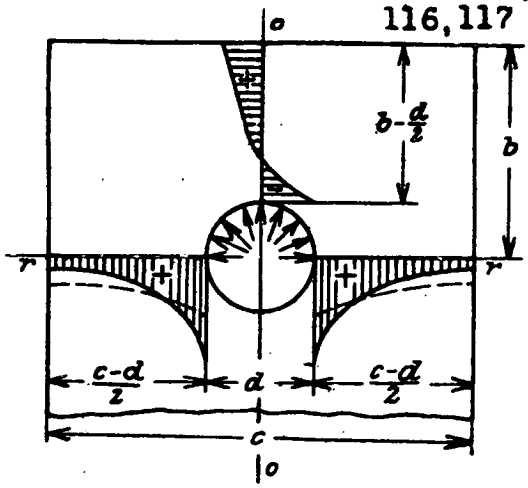

Fig.113 Distribution of stress in strap end.

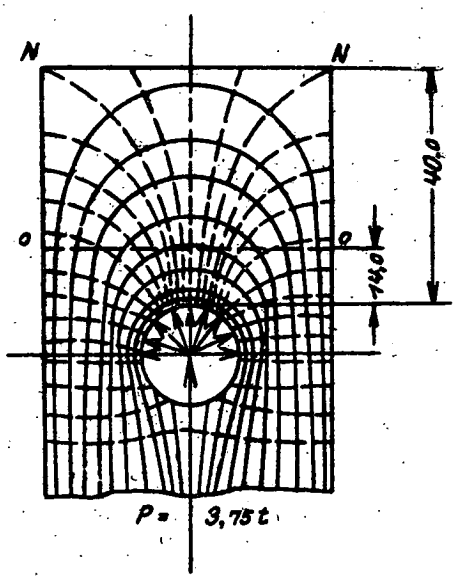

Fig.114 Shapes of lines of force in strap end with hole at upper edge.

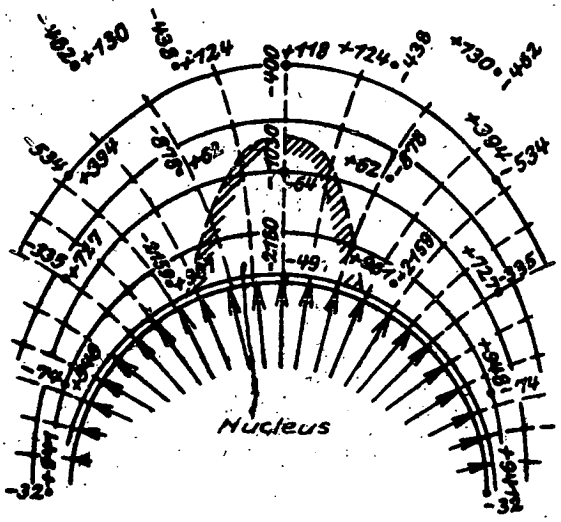

Fig.116 Zone of compression at strap edge above rivet hole.

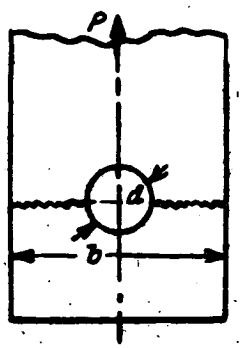

Fig.111 Tearing stress at critical section.

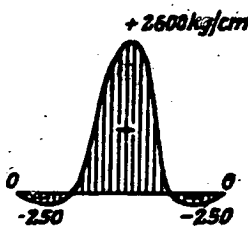

Fig.115 Stress distribution in strap end at upper edge.

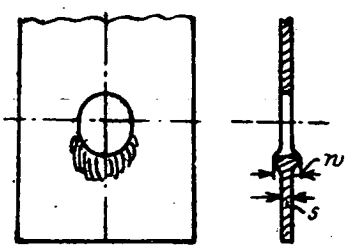

Fig.117 Ridge formation at hole edge caused by body of rivet.